IJST, Transactions of Mechanical Engineering, Vol. 39, No. M2, pp 367-387
Printed in The Islamic Republic of Iran, 2015

OPTIMAL SHAPE DESIGN FOR HEAT CONDUCTION USING SMOOTHED FIXED GRID FINITE ELEMENT METHOD AND MODIFIED FIREFLY ALGORITHM*

M. J. KAZEMZADEH-PARSI

Dept. of Mechanical Engineering, Shiraz Branch, Islamic Azad University, Shiraz, I. R. of Iran
Email: kazemzadeh@iaushiraz.ac.ir

Abstract– The present study is concerned with optimal shape determination of inhomogeneous and temperature dependent domains under steady state heat conduction. Such situations are important in many thermal design problems, especially in shape design of electronic components and chips. In the present paper, we formulate the shape optimization problem based on volume minimization of heat conductive material while limiting maximum temperature. The smoothed fixed grid finite element method which is a new approach based on the non-boundary-fitted meshes is used to obtain temperature field. The boundary parameterization technique using splines is also adopted to manipulate the shape variations. A modified version of the firefly algorithm which is a recently developed metaheuristic optimization technique is proposed as the optimizer. These modifications consist of adding memory, adding newborn fireflies and proposing a new updating formula. To evaluate the applicability of the proposed method five numerical examples are solved and the results are presented.

Keywords– Shape optimization, nonlinear heat conduction, smoothed fixed grid finite element method, metaheuristic optimization, firefly algorithm

1. INTRODUCTION

In the electronic components and chips, heat generated by the electrical elements is spread over the entire component by conduction and then transferred to the ambient via heat sinks or other devices. In such cases, design of the shape and size of the heat conducting medium have significant influence on the cooling performance of the equipment. In other words, in addition to the amount of the generated heat, the temperature distribution is dependent on the geometrical configuration of solid medium containing the heating element. A poor design may result in increasing the temperature of the devices, and even cause damage to the system components. Therefore, an optimal shape design for the component is definitely desirable and this is the problem considered in the present work.

Approximate (or numeric) solution of a Shape Optimization Problem (SOP) typically involves two major parts. The first part is a direct problem solver which provides information about the system behavior under various geometrical conditions and the second is an optimization algorithm that leads to a convergence of the iterative shape profile by updating the solutions. Therefore, SOPs can be categorized as variable domain problems in which the domain geometry has to be modified in each iteration to fulfill some requirements.

Among the several numerical methods used in the solution of the direct problem, the most appealing one in the context of variable domain problems is the Boundary Element Method (BEM). In the BEM, the domain discretization or mesh generation is not necessary, which makes BEM the most preferable method

*Received by the editors May 5, 2014; Accepted March 15, 2015.
**Corresponding author

for SOPs [1]. However, BEM has some drawbacks which limit its application in some problems, e.g. nonlinear on inhomogeneous materials. The other method is the Finite Element Method (FEM). The main drawback of FEM is that the mesh must be modified whenever the geometry of the problem is changed [2] and it is so cumbersome in variable domain problems. One approach to decrease FEM dependency on conventional mesh is to use Non-Boundary-Fitted Meshes (NBFM). By means of NBFMs in the analysis of variable domain problems, the analysis cost reduces significantly since there is no need to modify the mesh in iterations where the problem geometry is changed. The Fixed Grid Finite Element Method (FGFEM) [3 and 4] uses a fixed NBFM to perform a finite element analysis. In this method, the homogenization technique developed in [5] (as used in [3]) or a technique based on numerical integration (as used in [3]) is implemented to compute the element matrices. However, the homogenization procedure decreases the solution accuracy whereas numerical integration increases computational costs [4]. In the present work, the Smoothed Fixed Grid Finite Element Method (SFGFEM), which was previously proposed by the author in [6] is used to obtain the solution of direct problem. This method is based on the NBFMs and its main objective is to improve the accuracy of the formulation of the boundary intersecting elements. To tackle this, the gradient smoothing technique is used to evaluate domain integrals over the internal parts of the boundary intersecting elements. The gradient smoothing technique has been previously used in the smoothed finite element method [7]. The most interesting feature of this technique is simplification of integration over internal parts of the boundary intersecting elements. In the SFGFEM, the domain integrals are transformed into line integrals over the edges of smoothing cells and this will reduce the computational costs significantly. The SFGFEM has been previously used for the solution of inverse geometry problems [6, 8 and 9], unconfined flow problems in porous domains [10 and 11] and free surface potential flow problems [12].

Optimization appears in many real world problems and a considerable amount of work has been done in developing efficient algorithms for solving optimization problems. Classical optimization algorithms normally work well for smooth problems and use the gradient information which is difficult to obtain. In addition, the classical methods may converge to local optimum points. Thus, to overcome these difficulties, the gradient-free algorithms may be preferred. One class of derivative free techniques consists of nature inspired metaheuristic optimization algorithms. The vast majority of these algorithms have been derived from the behavior of biological or physical systems in nature [13]. These techniques have increased in popularity in recent years because of their ability to deal with complex optimization problems which are otherwise difficult to solve. The most popular methods are genetic algorithm [14], evolutionary strategies [15], evolutionary programming [16], particle swarm optimization [17], differential evolution [18], ant colony optimization [19], honey bee algorithm [20], bee algorithm [21], artificial bee colony [22], cuckoo search [23], hunting search [24], bat algorithm [25], firefly algorithm [26] and krill herd algorithm [27]. Besides bio inspired algorithms, there are nature inspired algorithms that mimic physical phenomena such as simulated annealing [28], harmony search [29], big bang-big crunch [30], charged system search [31], spiral optimization [32], biogeography based optimization [33], teaching learning algorithm [34] and ray optimization [35].

Firefly Algorithm (FA) is a recently developed, promising, metaheuristic optimization technique originally proposed by [36]. The FA is based on the idealized behavior of the flashing characteristics of fireflies. Based on Yang's works, the FA is very efficient in finding the global optima with high success rates [26]. It is also shown, using various test functions, that the FA is superior to both PSO and GA in terms of both efficiency and success rate [26]. For a review on the literature of FA refer to [37, 38 and 39]. After first presentation of the FA in [36] some modifications were proposed by different researchers; for example refer to [40, 41 and 42]. To continue this way, in the present work, some basic modifications are introduced in the original FA to improve its performance [43 and 44]. These modifications consist of: i)

adding a kind of memory to transfer some information obtained in each iteration to the next one, ii) adding newborn fireflies to explore extensively the search space for global optimum point and iii) introducing a new updating formula to reduce wandering motion of fireflies.

To evaluate the applicability of the proposed method in solution of SOPs five numerical examples are solved and the results are presented. The results show that a combination of the SFGFEM and the modified FA can be used effectively in the solution of shape optimization problems in heat conduction. The remaining part of this article deals firstly with solution of direct problem using SFGFEM and is followed by a brief review of the basics of the FA and a detailed description of the proposed modifications. After a brief note on the constraint handling approach, the numerical examples are solved and the results are presented. Finally the article ends with conclusions and references.

2. SHAPE OPTIMIZATION IN HEAT CONDUCTION

In the SOPs, it is assumed that the geometric shape of some parts of the domain boundary is unknown *a-priori* and must be obtained in the optimization process to minimize/maximize objective function subjected to constraints. Consider a general steady state conductive heat transfer occurred on a bounded domain Ω with boundary $\partial\Omega$ (refer to Fig. 1). Also, assume the domain consists of an inhomogeneous material with temperature dependent thermal conductivity. The temperature field $T(\mathbf{x})$ satisfies the following governing equation and boundary conditions,

$$\nabla\cdot\left[k(\mathbf{x},T)\nabla T(\mathbf{x})\right]+f(\mathbf{x})=0 \qquad \mathbf{x}\in\Omega \tag{1}$$

$$\left[-k(\mathbf{x},T)\nabla T(\mathbf{x})\right]\cdot\mathbf{n}=\bar{q} \qquad \mathbf{x}\in\Gamma_N \tag{2}$$

$$T(\mathbf{x})=\bar{T} \qquad \mathbf{x}\in\Gamma_D \tag{3}$$

where $f(\mathbf{x})$ is the body heat generation density and $k(\mathbf{x},T)$ is the thermal conductivity of the media which, in general, is a function of position and temperature. Γ_N and Γ_D are Neumann and Dirichlet boundaries, respectively. $\bar{q}$ and $\bar{T}$ are the prescribed heat flux and prescribed temperature, respectively and $\mathbf{n}$ is the unit outward normal vector. For direct problems, the geometry of the domain is assumed to be known and the temperature distribution over the entire problem domain can be determined directly. In the SOPs, the shape of the boundary Γ_U (see Fig. 1) is unknown *a-priori* and must be determined in the optimization process.

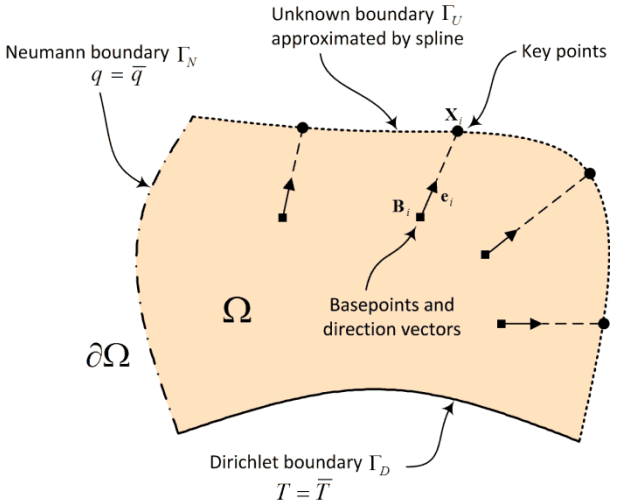

Fig. 1. Schematic representation of heat conductive domain, boundary conditions and unknown boundary parameterization

In order to obtain an approximate solution for SOP, the unknown boundary Γ_U is parameterized by a set of N_p shape parameters (or design variables) and a solution is pursued in a finite dimensional search space. Each distinct point in this search space represents a candidate shape for Γ_U. A direct problem can then be solved to obtain the corresponding temperature field. In the present work, the unknown boundary is approximated by a cubic spline passed through a set of key points to form a smooth boundary. As shown in Fig. 1, the location of each key point $\mathbf{X}_i$ is represented using a base point $\mathbf{B}_i$ and a direction vector $\mathbf{e}_i$ as

$$\mathbf{X}_i = \mathbf{B}_i + r_i \mathbf{e}_i \qquad i = 1,2,\cdots,N_p \tag{4}$$

where N_p is the number of key points and r_i is the shape parameter corresponding to the i th key point. In this work, the base points $\mathbf{B}_i$ and direction vectors $\mathbf{e}_i$ are assumed constant and therefore the unknown boundary Γ_U is parameterized based on the following unknown shape parameter vector $\mathbf{P}$.

$$\mathbf{P} = [r_1, r_2, \ \ldots, \ r_{N_p}] \tag{5}$$

The optimization problem in the present work is defined as searching for optimum distribution of minimum amount of conductive material in such a manner that the temperature of the hottest point of the domain remains below a specified allowable value. Therefore, the objective function f is defined as the area of the two dimensional domain $\Omega(\mathbf{P})$ subjected to the following constraint.

$$g(\mathbf{P}) = T_{\max} - T_{all} \le 0 \tag{6}$$

where $T_{\max}$ and T_{all} are the maximum and allowable temperature, respectively.

3. SMOOTHED FIXED GRID FINITE ELEMENT METHOD

A typical NBFM is shown in Fig. 2. The intersection of elements with boundaries produces three types of elements, Internal Elements (IE), External Elements (EE) and Boundary Intersecting Elements (BIE). The IEs and BIEs are used in the solution of direct problem and are considered as active elements. The nodes located on these active elements are also considered as active nodes.

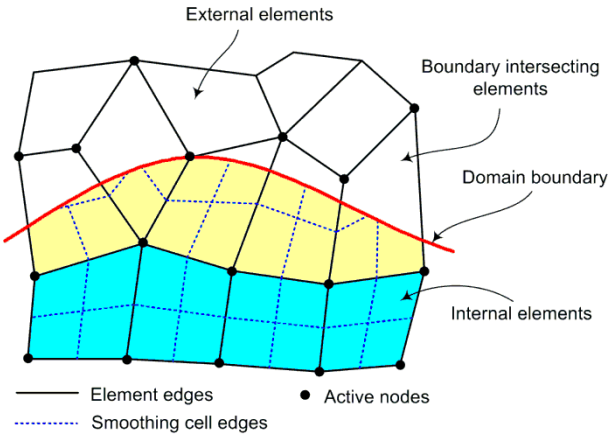

Fig. 2. Classification of elements and nodes in a typical non-boundary-fitted mesh and smoothing cells

Approximated temperature field T^h over the active elements can be written in terms of temperatures at the active nodes as:

$$T^h(\mathbf{x}) = \mathbf{N}\mathbf{T} \tag{7}$$

where $\mathbf{N}$ is the shape function vector and $\mathbf{T}$ is the nodal temperature vector. In the SFGFEM, the gradient smoothing technique is used to evaluate the gradient of the field variable. In this approach, each

element is divided into smoothing cells and the gradient of field variable is obtained using a smoothing operator [7]. The smoothing cells of IEs and BIEs are schematically presented in Fig. 2. Considering ∇T^h as the gradient of approximated temperature field, the smoothed temperature gradient in smoothing cell S denoted by $\tilde{\nabla} T_S^h$ can be defined as:

$$\tilde{\nabla} T_S^h = \int_{\Omega_S} \nabla T^h \, \phi_S \, d\Omega \tag{8}$$

where Ω_S is the domain of smoothing cell S and $\phi_S(\mathbf{x})$ is the smoothing kernel defined for cell S. Integration by parts for the right side of Eq. (8) leads to:

$$\tilde{\nabla} T_S^h = -\int_{\Omega_S} T^h \, \nabla \phi_S \, d\Omega + \int_{\Gamma_S} T^h \, \phi_S \, \mathbf{n} \, d\Gamma \tag{9}$$

where Γ_S is the boundary of smoothing cell S and $\mathbf{n}$ is the unit outward normal vector on Γ_S. A piecewise constant smoothing kernel is applied here as follows:

$$\phi_S(\mathbf{x}) = \begin{cases} 1/A_S & \mathbf{x} \in \Omega_S \\ 0 & \mathbf{x} \notin \Omega_S \end{cases} \tag{10}$$

where A_S is the area of the smoothing cell S. By substitution of $\phi_S(\mathbf{x})$, the smoothed temperature gradient over smoothing cell S is obtained as:

$$\tilde{\nabla} T_S^h = \frac{1}{A_S} \int_{\Gamma_S} T^h \, \mathbf{n} \, d\Gamma \tag{11}$$

Note that in Eq. (11) the gradient of the field variable is obtained via a line integration along the edges of smoothing cell. Substituting Eq. (7) in Eq. (11), the smoothed temperature gradient at smoothing cell S can be presented as:

$$\tilde{\nabla} T_S^h(\mathbf{x}) = \tilde{\mathbf{B}}_S \mathbf{T} \tag{12}$$

$$\tilde{\mathbf{B}}_S = \frac{1}{A_S} \int_{\Gamma_S} \mathbf{n} \, \mathbf{N} \, d\Gamma \tag{13}$$

where $\tilde{\mathbf{B}}_S$ is the smoothed gradient matrix.

Now, converting the differential equation and natural boundary conditions given in Eqs. (1 and 2) to the integral weak form, introducing the interpolation equations Eqs. (7 and 12) and using the Galerkin method [45], the discrete form of governing equations can be represented as:

$$\mathbf{K}(\mathbf{T})\mathbf{T} = \mathbf{R} \tag{14}$$

$$\mathbf{K}(\mathbf{T}) = \int_{\Omega} k(\mathbf{x}, T) \tilde{\mathbf{B}}^T \tilde{\mathbf{B}} d\Omega, \quad \mathbf{R} = \int_{\Omega} f(\mathbf{x}) \mathbf{N}^T d\Omega + \int_{\Gamma_N} \bar{q} \mathbf{N}^T d\Gamma \tag{15}$$

Calculation of the conductivity matrix $\mathbf{K}$ in Eq. (15) requires area integration over the problem domain Ω. This integration can be obtained by integration over entire IEs and internal parts of BIEs. On the other hand, assume constant thermal conductivity in each smoothing cell and note that the smoothed gradient matrix $\tilde{\mathbf{B}}_S$ is also a constant matrix within each smoothing cell, the conductivity matrix $\mathbf{K}$ can be obtained as follows:

$$\mathbf{K}(\mathbf{T}) = \sum_{IE} \sum_{S} \left(k(\mathbf{x}_S, T_S)\, A_S\, \widetilde{\mathbf{B}}_S^T\, \widetilde{\mathbf{B}}_S \right) + \sum_{BIE} \sum_{S} \left(k(\mathbf{x}_S, T_S)\, A_S\, \widetilde{\mathbf{B}}_S^T\, \widetilde{\mathbf{B}}_S \right) \tag{16}$$

where A_S, $\mathbf{x}_S$ and T_S are area, centroidal coordinate and centroidal temperature of the internal part of the smoothing cell S, respectively. The most interesting feature of the foregoing approach is that the area integrals are converted to the line integrals along the edges of the smoothing cells. This feature facilitates the usage of NBFMs, because in these meshes the internal part of BIEs usually has a general polygonal shape and computation of area integrals is not so trivial. The other advantage of this method is the less sensitivity with respect to geometric shape of the elements, as no geometric mapping for integration is used [7].

In general, conductivity matrix $\mathbf{K}$ is a function of temperature and Eq. (14) is a nonlinear system of algebraic equation. In the present work, the direct iteration method [45] is used for the iterative solution of this equation. In this method, the process is started from an initial guess, $\mathbf{T}^0$, for the temperatures and updated according to the following scheme.

$$\mathbf{K}(\mathbf{T}^r)\mathbf{T}^{r+1} = \mathbf{R} \tag{17}$$

where $\mathbf{T}^r$ denotes the solution at r th iteration. The iteration is continued until the difference between $\mathbf{T}^r$ and $\mathbf{T}^{r+1}$ reduces to an allowable error tolerance.

4. FIREFLY ALGORITHM

FA is a recently developed population based optimization algorithm which is inspired by the flashing behavior of fireflies [26]. In the FA each firefly is attracted to the brighter fireflies, and at the same time they move randomly. The attractiveness is proportional to the brightness of the flashing light which decreases with distance. Therefore, the attractiveness is evaluated in the eye of the other fireflies and the light absorption characteristic of the surrounding swill cause reduction of light intensity and the attractiveness of the fireflies. The attractiveness β can be defined as follows:

$$\beta = \beta_0 e^{-\gamma r^2} \tag{18}$$

The light absorption coefficient γ can be considered as a constant representing a characteristic length scale of the problem. Initial light intensity β_0 is the attractiveness at $r = 0$. If the position of any two fireflies *i* and *j* is designed by $\mathbf{x}_i$ and $\mathbf{x}_j$ respectively, the Cartesian norm $r = \left\| \mathbf{x}_i - \mathbf{x}_j \right\|$ represents the distance between these fireflies. The updating formula for relocating any firefly *i* which is attracted by a brighter firefly *j* is as follows:

$$\mathbf{x}_i^{new} = \mathbf{x}_i + \beta(\mathbf{x}_j - \mathbf{x}_i) + \alpha\boldsymbol{\varepsilon} \tag{19}$$

where the second term is due to the attraction, while the third term is random walk. α is the randomization parameter and $\boldsymbol{\varepsilon}$ is a random vector within the search space. FA may share many similarities with PSO. In fact, it has been proved in [26] that when $\gamma \to \infty$, the FA will become an accelerated version of PSO, while when $\gamma \to 0$, the FA reduces to a version of random search algorithms.

5. MODIFIED FIREFLY ALGORITHM

In the present paper, three basic modifications are introduced in the original FA to improve its performance. These points are explained in detail in the following subsections.

a) Memory

In many metaheuristic optimization algorithms there exists a kind of memory which transfers some information from one iteration to the other. For example, in PSO the particle best and also the global best positions are retained in each iteration. This information is then used in the next iteration for updating of the particles. As another example, in the genetic algorithm, the offspring inherit the genes from their parents and then transfer them to the next generation via crossover operator. In this point of view, the original FA suffers from lack of memory and no specific information is transferred from one iteration to the other.

To further elucidate, consider a firefly which reaches a near optimum point in one iteration. This firefly will participate in the updating process to generate the next population. It will attract other fireflies but it has no more chance to do this in successive iterations because the position of this firefly will also be changed and its information lost. To overcome this point, it is necessary to let some high rank fireflies be transferred to the next iteration. In this approach, in each iteration, a number of the high rank fireflies (say m_1) are directly transferred to the next iteration with no change in their position. To do this practically, in each iteration, the updating operator is not applied on the first m high rank fireflies and therefore the rest of them (n-m_1 fireflies) participate in the updating process. This approach tends to fix the high rank fireflies and other fireflies explore the search space extensively for the global optimum point.

b) Newborn fireflies

Mutation operator is one of the cornerstones of the genetic algorithm. It prevents the algorithm from being trapped in local optimum points and plays the role of recovering the lost genetic materials. If crossover operator in the genetic algorithm is supposed to exploit the current solution to find better ones (intensification), mutation is supposed to help in the exploration of the whole search space (diversification). Therefore, the mutation operator maintains genetic diversity in the population and helps to escape from local minimum traps.

Unfortunately, no such mechanism was designed in the original FA. As the second modification, a similar notion is introduced in the FA via adding newborn fireflies. To manage this, in each iteration, some new fireflies (say m_2) are generated randomly within the search space and inserted into the population. To keep total number of fireflies constant it is necessary to remove m_2 fireflies from the population, which is done by removing the low ranked ones.

c) Updating formula

The updating formula of the original FA, presented in Eq. (19), changes the position of each firefly towards all of the brighter fireflies in a stepwise manner regardless of the value of objective function of this firefly during these steps. For a better explanation, the reader is referred to Fig. 3 which schematically represents the updating path of a firefly in a two dimensional search space with 11 fireflies. In this figure, the fireflies are labeled according to their objective functions. For example, the fireflies 1 to 5 are brighter than the firefly 6. As it is shown, using Eq. (19), the firefly 6 changes its position repetitively toward the fireflies 1 to 5 and eventually reaches its final position. It is worth noting that the objective function is not reevaluated in each step where the position of this firefly changes. Therefore, relocation of this firefly is based on its objective at its initial position. As it is shown schematically in Fig. 3, it seems that this firefly is wandering and follows a zigzag updating path. This behavior of the original FA decreases the overall performance of the algorithm.

To overcome this point, a simple updating formula is proposed to remove the wandering motion of the fireflies. In this approach, instead of moving each firefly toward the brighter ones in a stepwise manner, a representative point which shows the overall distribution of the brighter fireflies is defined at

first and then the firefly moves toward this point in only one step. In other words, the updating formula for any firefly *i* which is attracted by a set of brighter fireflies is proposed as follows:

$$\mathbf{x}_i^{new} = \mathbf{x}_i + \beta(\mathbf{p}_i - \mathbf{x}_i) + \alpha\boldsymbol{\varepsilon} \tag{20}$$

where $\mathbf{p}_i$ is the representative point that shows the overall distribution of the brighter fireflies. Various ideas can be invoked to define this representative point $\mathbf{p}_i$. The simplest one, which is used here, is to define the coordinates of the point $\mathbf{p}_i$ as the average of the coordinates of the brighter fireflies as follows:

$$\mathbf{p}_i = \frac{1}{i-1}\sum_{l=1}^{i-1}\mathbf{x}_l \tag{21}$$

A schematic representation of the above updating formula is shown in Fig. 4.

Based on the modifications described in the foregoing sections, a pseudo code is prepared and shown in Fig. 5.

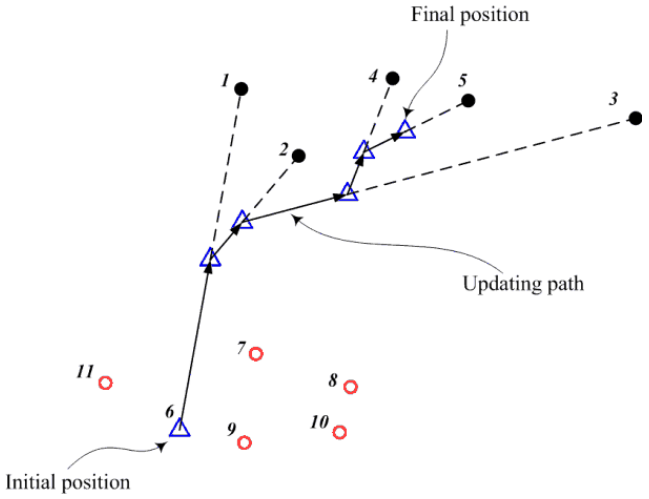

Fig. 3. Schematic representation of updating path of one firefly based on the original FA. The triangles show position of a firefly during updating process. The solid circles are brighter fireflies and the hollow circles are the rest of them.

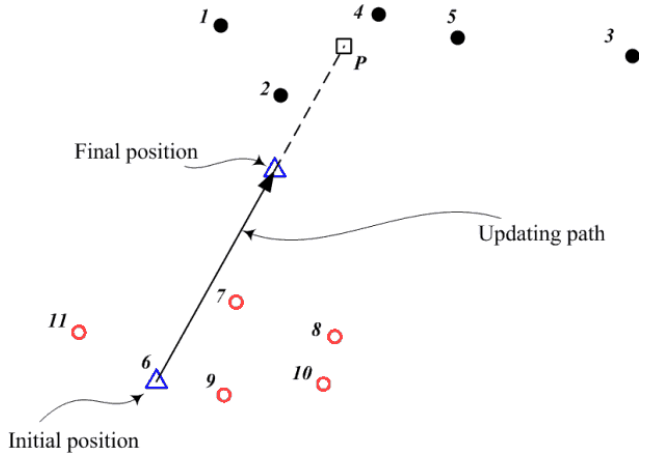

Fig. 4. Schematic representation of updating path of one firefly based on the proposed updating formula. The solid circles are brighter fireflies and the hollow circles are the rest of them. The square is the representative point of brighter fireflies

Define the upper bound U and lower bound L for the design variables
Generate an initial population of fireflies x_i (i=1 to n)
Evaluate the response function F_i for each firefly x_i
Sort the fireflies based on their response function
for *t=1 to Maximum iteration*
    $y_i=x_i$ (i=1 to n)
    for *i=m_1 to n-m_2*
        p=average of coordinates of fireflies which are brighter than x_i
        r=norm(x_i-p)
        $\beta = \beta_0 \times \exp(-\gamma r^2)$
        $\boldsymbol{\varepsilon} = (rand - 0.5) \times (\mathbf{U} - \mathbf{L})$
        $\mathbf{x}_i = \mathbf{x}_i + \beta(\mathbf{P} - \mathbf{x}_i) + \alpha\boldsymbol{\varepsilon}$
    next *i*
    Check the side constraints for firefly x_i
    for *i=m_2-k+1 to n*
        x_i=L+rand×(U-L)
    next *i*
    Evaluate the response function F_i only for the updated fireflies
    Sort the fireflies based on their response function
    Present the first firefly as the best solution obtained in this iteration
next *t*

Fig. 5. Pseudo code of the proposed modified firefly algorithm

6. CONSTRAINT HANDLING APPROACH

The most common approach in the metaheuristic optimization community to handle constraints is to use the penalty method. The basic idea of this method is to transform a constrained optimization problem into an unconstrained one by adding a certain value to the objective function based on the amount of constraint violation occurred in a certain solution. Such technique, which is known as the exterior penalty method, is one of the most popular methods of constraint handling in the evolutionary algorithms. A similar method is also used in the present work.

If the optimization problem consists of minimization of cost function f subjected to the inequality constraints $g_i \le 0, (i = 1 \text{ to } p)$ and equality constraints $h_i = 0, (i = 1 \text{ to } q)$, then in the penalty function approach, the constraints can be combined with the cost function into a response functional F defined as follows:

$$F = f + \sum_{i=1}^{p} \lambda_i (g_i^+)^2 + \sum_{i=1}^{q} \mu_i h_i^2 \tag{22}$$

$$g_i^+ = \max(g_i, 0) \tag{23}$$

where $\lambda_i >> 0$ and $\mu_i >> 0$ are the penalty coefficients. The penalty coefficients should be large enough to obtain a feasible solution and may depend on the specific optimization problem. By doing this, the constrained optimization problem is transformed into an unconstrained optimization problem which is simpler to solve.

7. NUMERICAL EXAMPLES

To evaluate the proposed method, five numeric examples are solved in this section. In the first two examples the material is considered as linear and homogeneous. In the third example, a nonlinear heat conduction with temperature dependent thermal conductivity is considered. In the fourth example, the

domain is divided into two zones and different thermal conductivity is assumed in each zone. In the last example, the shape of external boundary and also the dimensions of a high conductivity insert is obtained simultaneously. Each example is solved for different cases of allowable temperature and the results are presented. It must be noted that the SFGFEM is used as the direct solver and only a fixed NBFM is used to solve each example. In all of the following examples, the number of fireflies (n), number of high rank fireflies which are transferred to the next iteration (m_1) and number of newborn fireflies (m_2) are selected as $n=20$, $m_1=1$ and $m_2=1$, respectively. The algorithm is stopped after *100* iterations and totally *1900* function evaluations are performed in each case to obtain the results.

a) Example 1

As the first numerical example, consider the conductive heat transfer in the space between two parallel circular pipes which is filled with a filler material. By considering a two dimensional and symmetric field, a schematic representation of a half of problem domain and boundary conditions is presented in Fig. 6. As shown in this figure, a uniform heat flux of $\bar{q}=100$ is considered in the internal surface of the left pipe (face BC) and a prescribed temperature of $\bar{T}=0$ is considered in the internal surface of the right pipe (face DE). The faces AB, CD and EF have symmetric boundary condition. The geometric shape of face AF is unknown, but, its boundary condition is considered as insulated. A constant thermal conductivity of $k=1$ is considered for the entire domain. Finally, the shape optimization problem is defined as: determine the geometric shape of the face AF to minimize the volume (area, A, of the cross section) of the conductive material in such a way that the maximum field temperature $T_{\max}$ remains under the predefined allowable temperature T_{all}.

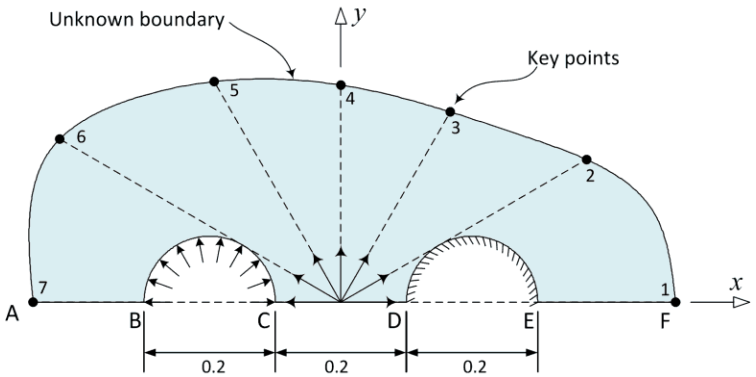

Fig. 6. Heat conductive domain, boundary conditions and unknown boundary parameterization for example 1

To solve this problem, the face AF is approximated using a cubic spline with seven key points. The coordinates of base points, components of direction vectors and lower and upper bounds of the shape parameters are presented in Table 1. As stated in Eq. (4), the coordinates of the key points can be defined using base points and direction vectors which are schematically shown in Fig. 6. A non-boundary-fitted mesh is generated based on the fixed boundaries and is shown in Fig. 7. The meshed area must be large enough to encompass the shape variations in the solution process. Three cases with different T_{all} are considered and the optimization problem is solved using the proposed algorithm in conjunction with the SFGFEM. The allowable temperature, T_{all}, maximum temperature, $T_{\max}$, and the domain area, A, are presented in Table 2 for each case. The obtained shapes of face AF are shown in Fig. 8 for each case and the temperature fields are also shown in Fig. 9. As presented in Table 2 the maximum temperatures are less than the allowable. It can also be seen that by decreasing the allowable temperature, more conductive

material is needed and its distribution tends to the left pipe. In other words, for a better protection against excessive temperature more conductive materials must be added near the left pipe.

Table 1. Base points, direction vectors and lower and upper bounds of the shape parameters considered in the example 1

Key point	B_x	B_y	e_x	e_y	r_L	r_U
1	0.0	0.0	1.000	0.000	0.350	0.600
2	0.0	0.0	0.866	0.500	0.300	0.693
3	0.0	0.0	0.500	0.866	0.173	0.693
4	0.0	0.0	0.000	1.000	0.150	0.600
5	0.0	0.0	-0.500	0.866	0.173	0.693
6	0.0	0.0	-0.866	0.500	0.300	0.693
7	0.0	0.0	-1.000	0.000	0.35	0.600

Table 2. Different cases considered in the example 1

Case	T_{all}	T_{max}	Area
A	45	44.926	0.266
B	55	54.845	0.155
C	65	64.867	0.116

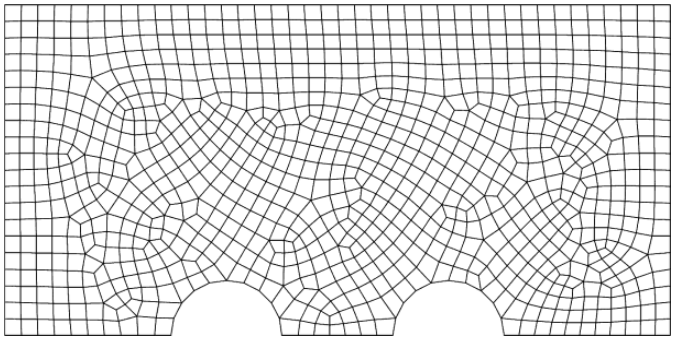

Fig.7. Non-boundary-fitted mesh used in the solution of example 1

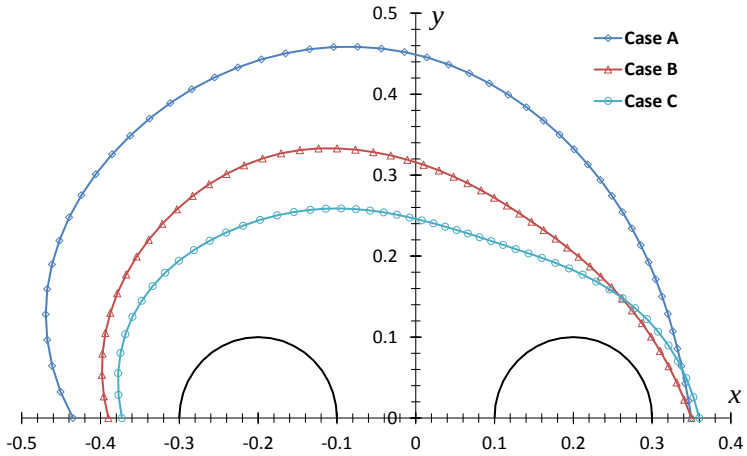

Fig. 8. Optimum shapes obtained for the example 1

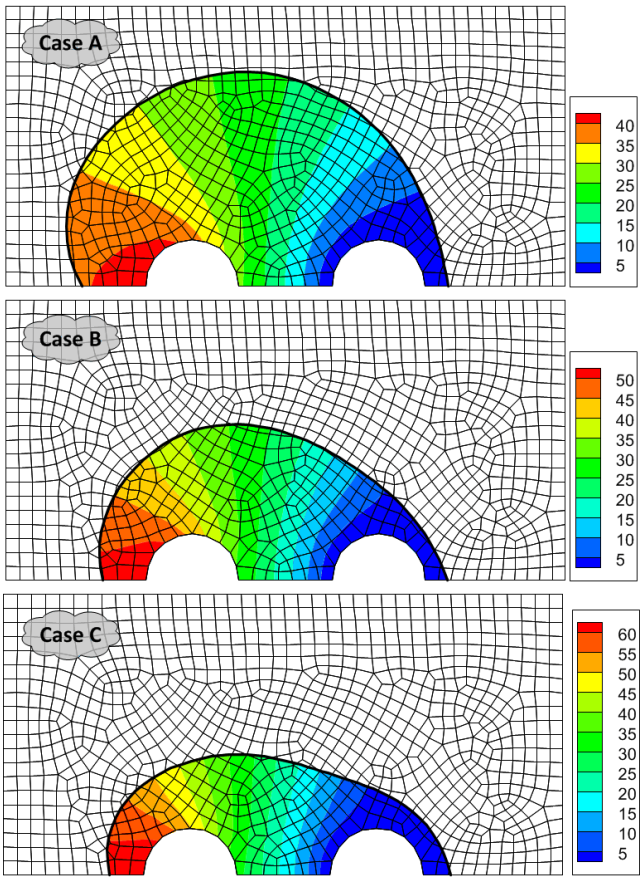

Fig. 9. Temperature distribution based on the optimum shapes for the example 1

b) Example 2

In this example consider the conductive heat transfer in a filler material located between two parallel flat surfaces as shown schematically in Fig. 10. Also, consider that the position of point D is fixed whereas point C can be selected from any point on the right side wall. Assume a uniform heat flux of $\bar{q}=100$ is applied on the left surface (face AD) and the right surface (face BC) is maintained at the constant temperature of $\bar{T}=0$. By considering a two dimensional and symmetric field, only half of the problem domain is modeled and symmetric boundary condition is applied on the face AB. The boundary condition of face DC is considered as insulated while its geometric shape is unknown *a priori*. In this example, a linear and homogeneous material with unit thermal conductivity ($k=1$) is considered and the shape optimization problem is defined as: determine the geometric shape of the unknown face DC to minimize the volume (area, *A*) of the filler material in such a way that the maximum field temperature $T_{\max}$ remains smaller than a predefined allowable temperature T_{all}.

The unknown face DC is approximated by a cubic spline with five key points. The coordinates of base points, components of direction vectors and lower and upper bounds of the shape parameters are presented in Table 3 and shown in Fig. 10. A NBFM is generated based on the fixed boundaries and the meshed area must be large enough to encompass the shape variations in the solution process. Five cases with different T_{all} are considered and the optimization problem is solved using the proposed algorithm. The allowable temperature, T_{all}, maximum temperature, $T_{\max}$, and the domain area, *A*, are presented in Table 4 for each case. The obtained boundary shapes of face DC are shown in Fig. 11 for each case and the temperature fields are also shown in Fig. 12. The results show that decreasing the allowable temperature will cause point C to move upward and more conductive material will be required to satisfy the temperature limit.

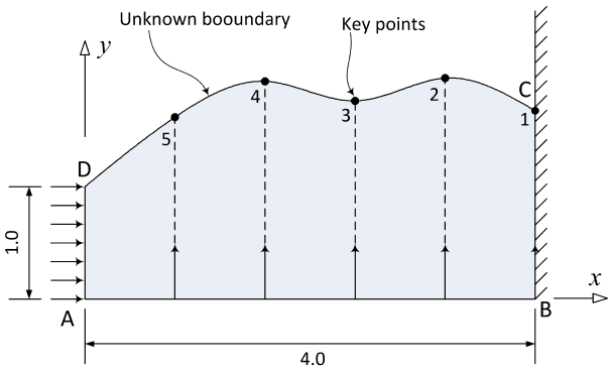

Fig. 10. Heat conductive domain, boundary conditions and unknown boundary parameterization for example 2

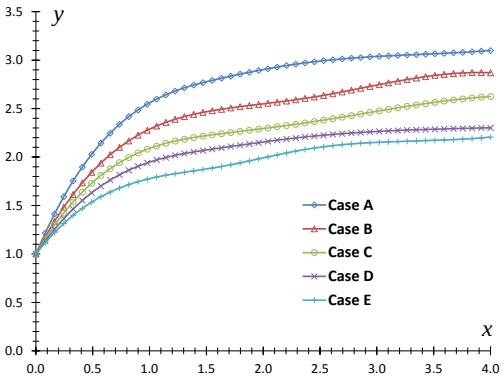

Fig. 11. Optimum shapes obtained for the example 2

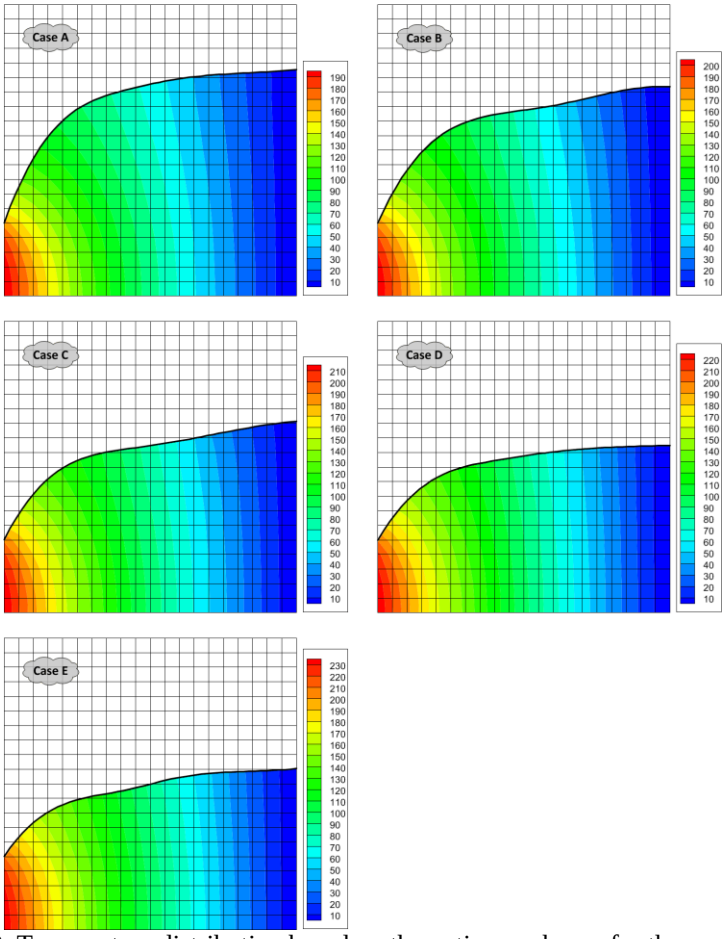

Fig. 12. Temperature distribution based on the optimum shapes for the example 2

Table 3. Base points, direction vectors and lower and upper bounds of the shape parameters considered in the example 2

Key point	B_x	B_y	e_x	e_y	r_L	r_U
1	4.0	0.0	0.0	1.0	1.0	4.0
2	3.2	0.0	0.0	1.0	1.0	4.0
3	2.4	0.0	0.0	1.0	1.0	4.0
4	1.6	0.0	0.0	1.0	1.0	4.0
5	0.8	0.0	0.0	1.0	1.0	4.0

Table 4. Different cases considered in the example 2

Case	T_{all}	T_{max}	Area
A	200	199.912	10.759
B	210	209.936	9.692
C	220	210.859	8.819
D	230	229.764	8.146
E	240	238.854	7.633

It is worth to note that a little wavy modes which can be observed in the boundary profiles in Fig. 11 are due to oscillatory nature of cubic splines. These waves will be reduced by increasing the accuracy of optimizer e.g. by increasing the population size or number of generations.

c) Example 3

The main goal of the third example is to evaluate the method in solution of nonlinear heat conduction problems. Consider the conductive heat transfer between two parallel flat surfaces where the geometry and boundary conditions are similar to the previous example. The unknown boundary, number of key points, base points and direction vectors are also the same. The thermal conductivity is considered here as a function of field temperature as follows:

$$k(T) = 1 + T/50 \tag{24}$$

The shape optimization problem of the present example is solved for five cases with different T_{all}. The allowable temperature, T_{all}, maximum temperature, $T_{\max}$, and the domain area, A, are presented in Table 5 for each case. The obtained boundary shapes of face DC are shown in Fig. 13 for each case and the temperature fields are also shown in Fig. 14.

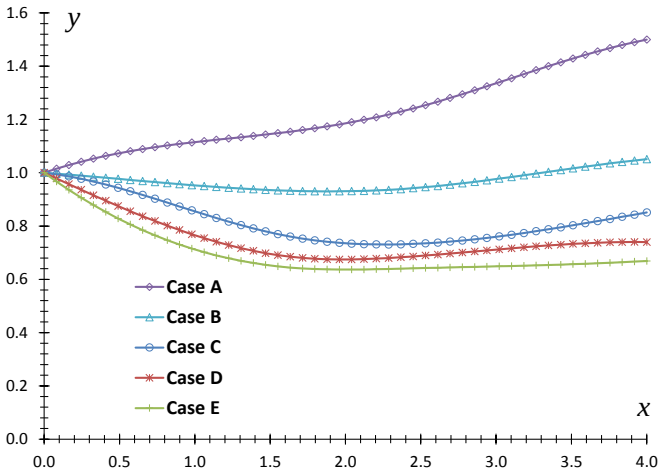

Fig. 13. Optimum shapes obtained for the example 3

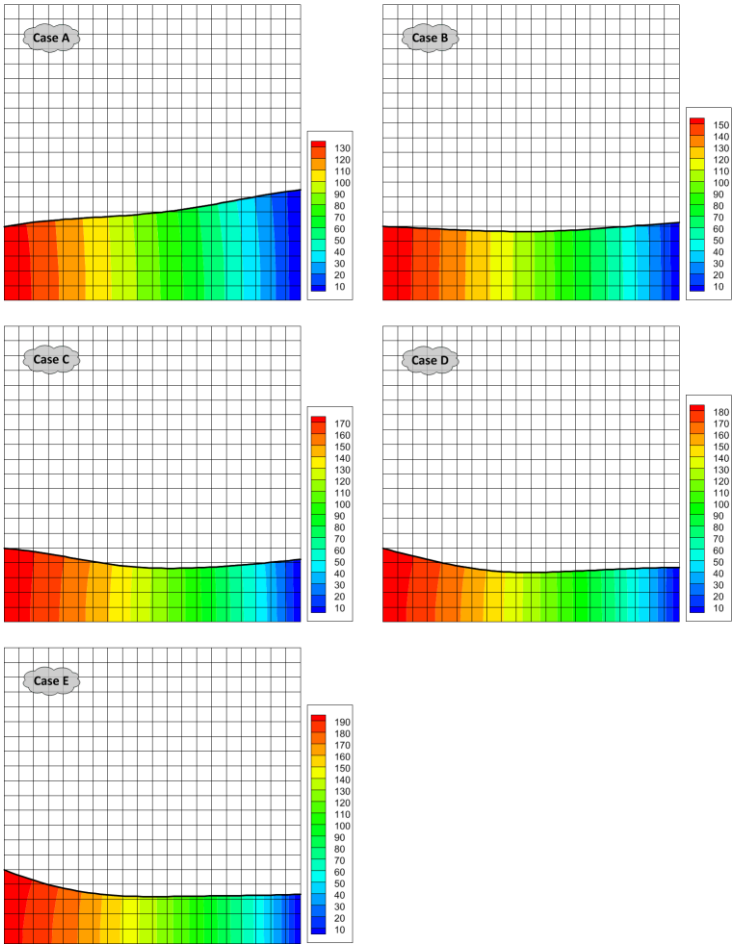

Fig. 14. Temperature distribution based on the optimum shapes for the example 3

Table 5. Different cases considered in the example 3

Case	T_{all}	T_{max}	Area
A	140	139.769	4.888
B	160	159.924	3.875
C	180	179.395	3.259
D	190	190.233	2.997
E	200	199.819	2.793

As mentioned in the previous example, a small wavy modes can be observed in the boundary profiles in Fig. 13 which are due to oscillatory nature of cubic splines. Increasing the accuracy of the optimizer will reduce these oscillations but the overall shape of the boundary will remain the same.

d) Example 4

In this example, the shape optimization problem for a zoned inhomogeneous domain is considered. Similar to the previous two examples, the conductive heat transfer between two parallel flat surfaces is also considered here and the geometry, boundary conditions, number of key points, base points and direction vectors are the same. As shown in Fig. 15, the domain is divided to two zones with different thermal conductivity $k_1 = 0.2$ and $k_2 = 20.0$.

The shape optimization problem of this example is also solved for four cases. The allowable temperature, T_{all}, maximum temperature, $T_{\max}$, and the domain area, A, are presented in Table 6 for each case. The obtained boundary shapes of face DC are shown in Fig. 16 for each case and the temperature fields are also shown in Fig. 17. As presented in Table 6 the maximum temperatures constraint is satisfied and by decreasing the allowable temperature, more conductive material is needed. In other words, for a

better protection against temperature rise more conductive materials must be added near heat source (left side wall).

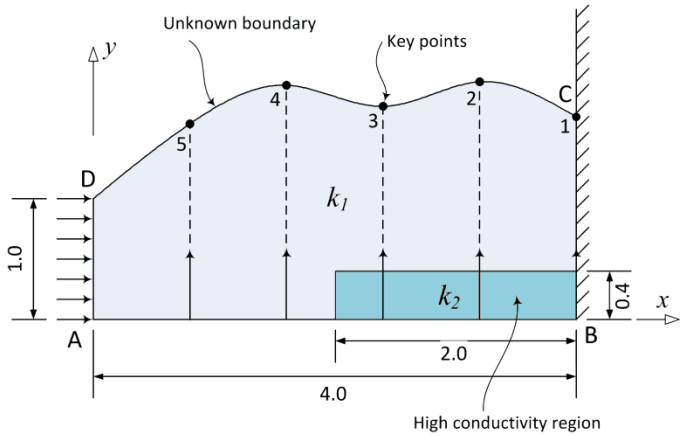

Fig. 15. Heat conductive domain, boundary conditions and unknown boundary parameterization for example 4

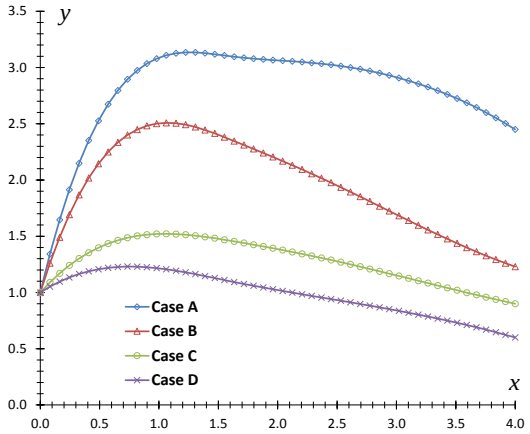

Fig. 16. Optimum shapes obtained for the example 4

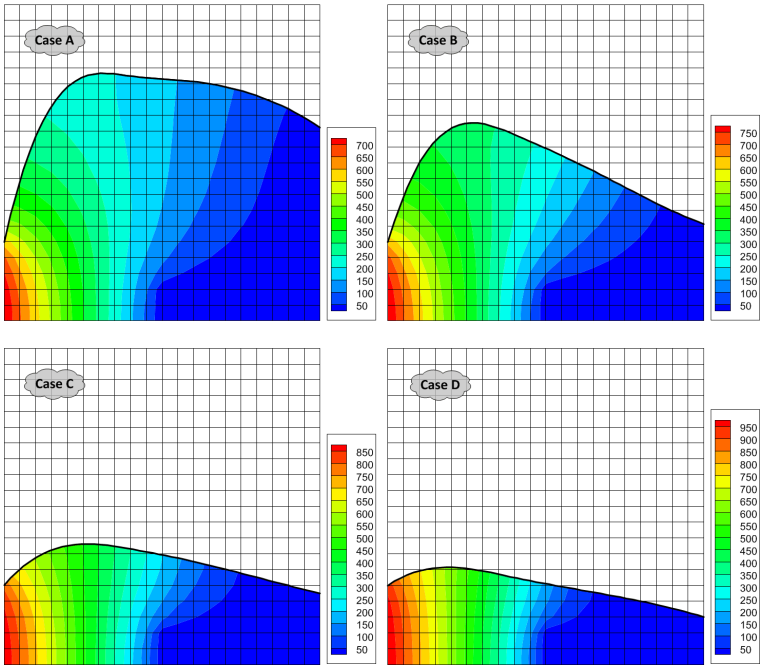

Fig. 17. Temperature distribution based on the optimum shapes for the example 4

Table 6. Different cases considered in the example 4

Case	T_{all}	T_{max}	Area
A	750	749.097	11.191
B	800	800.014	7.794
C	900	899.360	5.115
D	1000	1000.045	3.953

e) Example 5

In the last example, consider a heat generating device which must be protected from increase in temperature by transferring heat to a heat sink. To do this, a heat conducting medium must be designed to efficiently transfer the heat to the heat sink. A schematic representation of half of the problem domain (due to symmetry) is shown in Fig. 18. Heat is generated in a circular region centered at point B and the heat sink is located at the right side boundary CD. To increase the heat transfer rate, a high conductivity part of the rectangular shape is inserted in the medium and attached to the heat sink. The size (*a* and *b* according to Fig. 18) of this insert is also considered as unknown and must be obtained in the optimization process. The thermal conductivity of the domain is considered as $k_1 = 1.0$ except for the rectangular insert which is considered as $k_2 = 20.0$. In the present example, the volume (area) of the rectangular insert is considered as constant value of *1.5*. Therefore, the relation $b = 1.5/a$ must be considered in the shape design problem. A uniform heat generation rate of $f = 30.0$ is considered over circular region and a prescribed temperature of $\bar{T} = 0$ is considered for the heat sink (face CD). The face AC has symmetric boundary condition. In such circumstance, the shape optimization problem is defined as: determine the geometric shape of the face AD and dimension *a* of the insert to minimize the volume (area) of the conductive material in such a way that the maximum field temperature $T_{\max}$ remains under the predefined allowable temperature T_{all}.

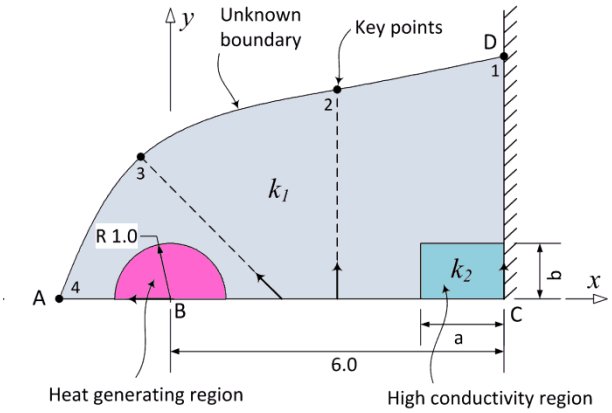

Fig. 18. Heat conductive domain, boundary conditions and unknown boundary parameterization for example 5

To solve this problem, the face AD is approximated using a cubic spline with four key points. The coordinates of base points, components of direction vectors and lower and upper bounds of the shape parameters are presented in Table 7 and are also shown in Fig. 18. The bound constraint for the size of insert is $0.5 \le a \le 3.0$. A non-boundary-fitted mesh is generated based on the fixed boundaries and is shown in Fig. 19. The meshed area must be large enough to encompass the shape variations in the solution process. Four cases with different T_{all} are considered and the optimization problem is solved using the proposed algorithm in conjunction with the SFGFEM. The allowable temperature, T_{all}, maximum temperature, $T_{\max}$, insert size, *a*, and the area, *A*, are presented in Table 8 for each case. The obtained shapes of face AD are shown in Fig. 20 for each case and the temperature fields are also shown in Fig. 21.

It is observed that the shape parameter corresponding to key point 4 converges to its lower bound and size *a* of the insert converges to its upper bound. This means that a horizontal rectangular insert behaves better than a vertical rectangular insert and to protect against temperature rise more conductive materials must be placed near the insert.

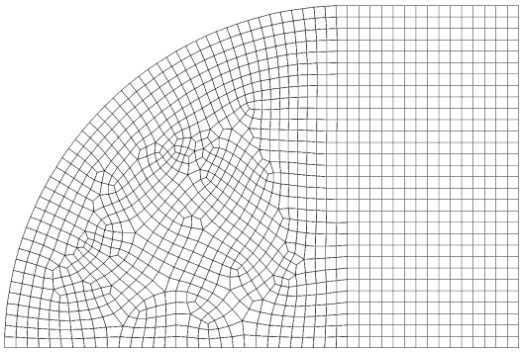

Fig. 19.Non-boundary-fitted mesh used in the solution of example 5

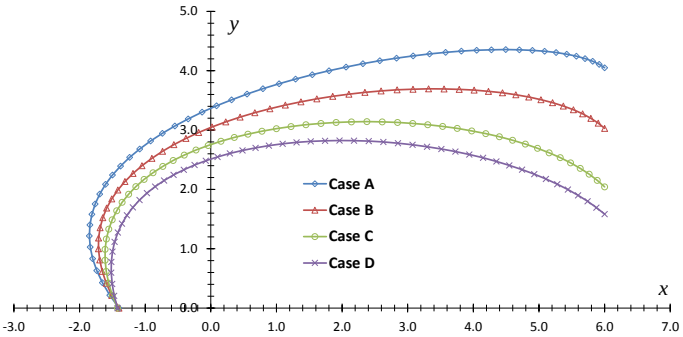

Fig. 20. Optimum shapes obtained for the example 5

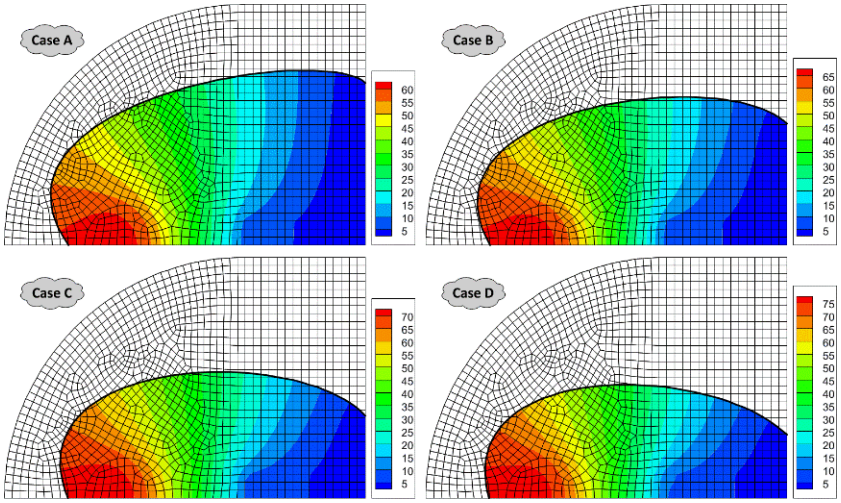

Fig. 21. Temperature distribution based on the optimum shapes for the example 5

Table 7. Base points, direction vectors and lower and upper bounds of the shape parameters considered in the example 5

Key point	B_x	B_y	e_x	e_y	r_L	r_U
1	6.0	0.0	0.000	1.000	1.582	5.7
2	3.0	0.0	0.000	1.000	2.545	5.7
3	2.0	0.0	-0.707	0.707	3.041	5.1
4	0.0	0.0	-1.000	0.000	1.400	3.0

Table 8. Different cases considered in the example 5

Case	T_{all}	T_{max}	a	Area
A	65	64.999	3.000	29.340
B	70	69.515	3.000	25.080
C	75	74.727	3.000	20.986
D	80	79.843	3.000	18.310

8. CONCLUSION

In the present work, the shape optimization problems in nonlinear heat conductions in inhomogeneous materials were considered. The boundary parameterization technique using splines was utilized to manipulate the variation of the domain boundary during the iterative process. Solution of direct problem is obtained using SFGFEM approach which is based on the non-boundary-fitted meshes. This method facilitates solution of variable domain problems since the mesh modification (or remeshing) is eliminated completely in the solution of direct problem. A modified version of the firefly algorithm is proposed here as the optimization algorithm in which three basic modifications were done to improve its performance. They were: adding memory, adding mutation and proposing a new updating formula. The memory stores valuable information in each iteration and transfers it to the next iteration. The mutation promotes diversification of the optimizer in searching of the entire solution space for potential optima. The proposed updating formula overcomes wandering motion of the fireflies. Some numerical examples were solved to evaluate the proposed method. In these examples, the effects of different boundary shapes, parameterizations and material properties on the solution of shape optimization problem were examined. It is believed that the use of the non-boundary-fitted meshes in conjunction with modified firefly algorithm simplified the solution of shape optimization problems and provides an effective engineering tool in thermal shape design problems.

Acknowledgements: The results presented in this paper are from a research project supported financially by Shiraz Branch, Islamic Azad University, Shiraz, Iran. Partial support of the author by the Shiraz Branch, Islamic Azad University is also appreciated.

REFERENCES

1. Huang, C. H. & Shih, C. C. (2006). A shape identification problem in estimating simultaneously two interfacial configurations in a multiple region domain. *Applied Thermal Engineering*, Vol. 26, pp. 77-88.
2. Lee, H. S., Kim, Y. H., Park, C. J. & Park, H. W. (1999). A new spatial regularization scheme for the identification of the geometric shape of an inclusion in a finite body. *International Journal for Numerical Methods in Engineering*, Vol. 46, pp. 973-992.
3. Garcia, M. J. & Steven, G. P. (1999). Fixed grid finite elements in elasticity problems. *Engineering Computations*, Vol. 16, pp. 145-164.
4. Daneshmand, F. & Kazemzadeh-Parsi, M. J. (2009). Static and dynamic analysis of 2D and 3D elastic solids using the modified FGFEM. *Finite Elements in Analysis and Design*, Vol. 45, pp. 755-765.
5. Bendsoe, M. P. & Kikuchi, N. (1988). Generating optimal topologies in structural design using a homogenization method. *Computer Methods in Applied Mechanics and Engineering*, Vol. 71, pp. 197-224.
6. Kazemzadeh-Parsi, M. J. & Daneshmand, F. (2009). Solution of geometric inverse heat conduction problems by smoothed fixed grid finite element method. *Finite Elements in Analysis and Design*, Vol. 45, pp. 599-611.
7. Liu, G. R., Dai, K. Y. & Nguyen, T. T. (2007). A smoothed finite element for mechanics problems. *Computational Mechanics*, Vol. 39, pp. 859-877.

8. Kazemzadeh-Parsi, M. J. & Daneshmand, F. (2010). Cavity shape identification with convective boundary conditions using non-boundary-fitted meshes. *Numerical Heat Transfer, Part B: Fundamentals*, Vol. 57, -pp. 283-305.
9. Kazemzadeh-Parsi, M. J. & Daneshmand, F. (2013). Inverse geometry heat conduction analysis of functionally graded materials using smoothed fixed grid finite elements. *Inverse Problems in Science and Engineering*, Vol. 21, No. 2, pp. 235-250.
10. Kazemzadeh-Parsi, M. J. & Daneshmand, F. (2012). Unconfined seepage analysis in earth dams using smoothed fixed grid finite element method. *International Journal for Numerical and Analytical Methods in Geomechanics*, Vol. 36, pp. 780-797.
11. Kazemzadeh-Parsi, M. J. & Daneshmand, F. (2013). Three dimensional smoothed fixed grid finite element method for the solution of unconfined seepage problems. *Finite Elements in Analysis and Design*, Vol. 64, pp. 24-35.
12. Kazemzadeh-Parsi, M. J. (2014). Numerical flow simulation in gated hydraulic structures using smoothed fixed grid finite element method. *Applied Mathematics and Computation*, Vol. 246, pp. 447-459.
13. Talbi, E. (2009). Metaheuristics: from design to implementation, *John Wiley & Sons*, Hoboken, New Jersey.
14. Goldberg, D. (1989). *Genetic algorithms in search optimization and machine learning*. Addison-Wesley.
15. Back, T., Hoffmeister, F. & Schwefel, H. (1991). A survey of evolution strategies. *Proceedings of the Fourth International Conference on Genetic Algorithms and their Applications*, San Mateo, CA, pp. 2-9.
16. Fogel, L. (1994). *Evolutionary programming in perspective: The top-down view*. Computational Intelligence: Imitating Life, edited by Zurada. J.M., Marks, Jr., R., and Robinson, C., IEEE Press, Piscataway, NJ, USA.
17. Eberhart, R.C., and Kennedy, J. (1995). A new optimizer using particle swarm theory. *Proceedings of the sixth international symposium on micro machine and human science*, Nagoya, Japan.
18. Storn, R. & Price, K. (1995). Differential evolution - A simple and efficient adaptive scheme for global optimization over continuous spaces. Technical Report TR-95-012, Berkeley, CA, USA.
19. Dorigo, M., Maniezzo, V. & Colorni, A. (1996). The ant system: optimization by a colony of cooperating agents. *Systems, Man, and Cybernetics, Part B: Cybernetics, IEEE Transactions*, Vol. 26, Vol. 1, pp. 29-41.
20. Nakrani, S. & Tovey, C. (2004). On honey bees and dynamic server allocation in internet hosting centers. *Adaptive Behavior*, Vol. 12, pp. 223-240.
21. Pham, D. T., Ghanbarzadeh, A., Koc, E., Otri, S., Rahim, S. & Zaidi, M. (2005). The bees algorithm. Technical Note, *Manufacturing Engineering Center*, Cardiff University.
22. Karaboga, D. (2005). An idea based on honey bee swarm for numerical optimization. Technical Report, Erciyes University.
23. Yang, X. S. & Deb, S. (2009). Cuckoo search via Lévy flights. *Proceedings of the world congress on nature & biologically inspired computing* (NaBIC 2009), IEEE Publications, pp. 210-214.
24. Oftadeh, R., Mahjoob, M. J. & Shariatpanahi, M. (2010). A novel meta-heuristic optimization algorithm inspired by group hunting of animals: Hunting search. *Computers & Mathematics with Applications*, Vol. 60, No. 7, pp. 2087-2098.
25. Yang, X. S. (2010). A new metaheuristic bat-inspired algorithm. Nature inspired cooperative strategies for optimization NISCO edited by Gonzalez, J.R. et al., *studies in computational intelligence*, Vol. 284. Berlin: Springer, pp. 65-74.
26. Yang, X. S. (2010). *Nature-inspired metaheuristic algorithms*. 2nd edition, United Kingdom: Luniver Press.
27. Gandomi, A. H. & Alavi, A. H. (2012). Krill herd: A new bio-inspired optimization algorithm. *Communications in Nonlinear Science and Numerical Simulation*, Vol. 17, pp. 4831-4845.
28. Kirtrick, S., Gelatt, C. D. & Vecchi, M. P. (1983). Optimization by simulated annealing. *Science*, Vol. 220, (4598), pp. 671-680.

29. Geem, Z. W., Kim, J. H. & Loganathan, G. V. (2001). A new heuristic optimization algorithm: Harmony Search. *Simulation*, Vol. 76, No. 2, pp. 60-68.
30. Osman, K. & Erol, I. E. (2006). A new optimization method: Big Bang-Big Crunch. *Advanced Engineering Software*, Vol. 37, No. 2, pp. 106-111.
31. Kaveh, A. & Talatahari, S. (2010). A novel heuristic optimization method: charged system search. *Acta Mechanica*, Vol. 213, Nos. 3-4, pp. 267-289.
32. Tamura, K. & Yasuda, K. (2011). Spiral dynamics inspired optimization. *Journal of Advanced Computational Intelligence and Intelligent Informatics*, Vol. 15, No. 8, pp. 1116-1122.
33. Boussaid, I., Chatterjee, A., Siarry, P. & Ahmed-Nacer, M. (2012). Biogeography-based optimization for constrained optimization problems. *Computers & Operations Research*, Vol. 39, pp. 3293-3304.
34. Rao, R. V., Savsani, V. J. & Balic, J. (2012). Teaching-learning-based optimization algorithm for unconstrained and constrained real-parameter optimization problems. *Engineering Optimization*, Vol. 44, No. 12, pp. 1447-1462.
35. Kaveh, A. & Khayatazad, M. (2012). A new meta-heuristic method: Ray Optimization. *Computers and Structures*, Vol. 112-113, pp. 283-294.
36. Yang, X. S. (2009). Firefly algorithms for multimodal optimization in Stochastic Algorithms: Foundations and Applications. *SAGA, Lecture Notes in Computer Sciences*, Vol. 5792, pp. 169-178.
37. Fister, I., Fister Jr., I., Yang, X. S. & Brest, J. (2013). A comprehensive review of firefly algorithms. *Swarm and Evolutionary Computation*, Vol. 13, No. 1, pp. 34-46.
38. Yang, X. S. (2013). Multiobjective firefly algorithm for continuous optimization. *Engineering with Computers*, Vol. 29, No. 2, pp. 175-184.
39. Yang, X. S. (2014). Cuckoo search and firefly algorithm: Theory and applications. *Studies in Computational Intelligence*, Vol. 516, Springer.
40. Wang, G., Guo, L., Duan, H., Liu, L. & Wang, H. (2012). A modified firefly algorithm for UCAV path planning. *International Journal of Hybrid Information Technology*, Vol. 5, No. 3, pp. 123-144.
41. Coelho, L. D. S. & Mariani, V. C. (2012). Firefly algorithm approach based on chaotic Tinkerbell map applied to multivariable PID controller tuning. *Computers & Mathematics with Applications*, Vol. 64, No. 8, pp. 2371-2382.
42. Gandomi, A. H., Yang, X. S., Talatahari, S. & Alavi, A. H. (2013). Firefly algorithm with chaos. *Communications in Nonlinear Science and Numerical Simulation*, Vol. 18, No. 1, pp. 89-98.
43. Kazemzadeh-Parsi, M. J., Daneshmand, F., Ahmadfard, M. A., Adamowski, J. & Martel, R. (2015). Optimal groundwater remediation design of pump and treat systems via a simulation-optimization approach and firefly algorithm. *Engineering Optimization*, Vol. 47, No. 1, pp. 1-17.
44. Kazemzadeh-Parsi, M. J. (2014). A modified firefly algorithm for engineering design optimization problems. *Iranian Journal of Science and Technology*, Vol. 38, pp. 403-421.
45. Reddy, J. N. (2006). *An introduction to the finite element method*. Third edition, McGraw-Hill, New York.